Curcumin Binds to $A\beta_{1-40}$ Peptides and Fibrils Stronger Than Ibuprofen and Naproxen

Journal:	*The Journal of Physical Chemistry*
Manuscript ID:	jp-2012-02506a.R2
Manuscript Type:	Article
Date Submitted by the Author:	01-Aug-2012

Complete List of Authors:	Ngo, Son Tung; Institute of Computational Science and Technology, Life Science Li, Mai Suan; Institute of Physics, Polish Academy of Sciences,

Curcumin binds to Aβ_{1-40} peptides and fibrils stronger than ibuprofen and naproxen

Son Tung Ngo[†,‡] and Mai Suan Li[*,‡]

Institute for Computational Science and Technology, 6 Quarter, Linh Trung Ward, Thu Duc District, Ho Chi Minh City, Vietnam, and Institute of Physics, Polish Academy of Sciences, Al. Lotnikow 32/46, 02-668 Warsaw, Poland

E-mail: masli@ifpan.edu.pl

Abstract

Binding of curcumin, naproxen and ibuprofen to Aβ_{1-40} peptide and its fibrils is studied by docking method and all-atom molecular dynamics simulations. The Gromos96 43a1 force field and simple point charge model of water have been used for molecular dynamics simulations. It is shown that if the receptor is a monomer then naproxen and ibuprofen are bound to the same place that is different from the binding position of curcumin. However all of three ligands have the same binding pocket in fibrillar structures. The binding mechanism is studied in detail showing that the van der Waals interaction between ligand and receptor dominates over the electrostatic interaction. The binding free energies obtained by the molecular mechanic-Poisson Boltzmann surface area method indicate that curcumin displays higher binding affinity than non-steroidal anti-inflammatory drugs. Our results are in good agreement with the experiments.

[*]To whom correspondence should be addressed
[†]Institute for Computational Science and Technology, Institute of Physics
[‡]Institute of Physics

Introduction

Alzheimer's disease (AD) is the most common form of dementia among the senior population that is increasing substantially as populations age.[1] The patient with AD will lose memory,[2] decay language,[3] and have problems with visual spatial search[4] *etc*. AD may be pathologically characterized by progressive intracerebral accumulation of beta amyloid ($A\beta$) peptides[5] and tau protein.[6] However, genetic and pathological evidences strongly support the first hypothesis.[7,8] The $A\beta$ peptides are proteolytic by-products of the amyloid precursor protein and are most commonly composed of 40 ($A\beta_{1-40}$) and 42 ($A\beta_{1-42}$) amino acids. $A\beta$ peptides appear to be unstructured in monomer state but aggregate to form fibrils with an ordered cross-β-sheet pattern.[9–12] Increasing evidence from recent studies indicates that both soluble oligomers and mature fibrils are the toxic agents.[5,13,14]

Presently, there is no cure or treatment for AD, and significant effort has, therefore, been made to find efficient drugs to cope with it. One of the promising approaches is to inhibit misfolding and reverse aggregation of amyloid peptides.[7,15] A large number of potential $A\beta$ fibrillogenesis inhibitors have been proposed including polyamines,[16,17] metal chelators,[18] chaperones,[19] carbohydrate-containing compounds,[20,21] osmolytes,[22] short peptides[23–27] and RNA aptamers[28] etc.[15,29,30] Nutraceuticals, which are natural products or extracts therefrom, as shown by preclinical and certain clinical studies, might be of value as AD therapeutic agents.[15,31]

Curcumin (diferulomethane), a low molecular weight molecule derived from the rhizome of curcuma longa, can inhibit $A\beta$ aggregation.[32,33] Although this potentially important lead is under phase II clinical trial,[34] the nature of its binding to $A\beta$ peptides and fibrillar structures has not been understood at the atomic level. Experimental and epidemiological studies suggest that non-steroidal anti-inflammatory drugs (NSAID) naproxen and ibuprofen are potential candidates to control $A\beta$ aggregation. Their chronic consumption can not only suppress inflammatory targets, which could contribute to neuroprotection, but also slow down amyloid deposition by mechanisms that remain unclear.[35–38] Molecular dynamics (MD) simulations of anti-aggregation effect of ibuprofen and naproxen were carried out by Klimov et al[39–42] who showed that in agreement

with the experiments[35] ibuprofen displays lower Aβ binding affinity than naproxen. However, the binding free energies ΔG_{bind} of ibuprofen and naproxen to Aβ peptides and their mature fibrils that can be directly compared with experimental values of inhibition constants[33,35] have not been estimated.

The experiments of Yang *et al*[32] have shown that curcumin, which is non-toxic and able to cross the blood-brain barrier due to its high hydrophobicity, can interfere with Aβ oligomerization better than ibuprofen and naproxen. So, it is worth to address this problem by computer simulations to shed more light on the binding nature of these ligands. Moreover, ΔG_{bind} of curcumin to Aβ monomer and aggregates has not been also computed. As shown by the experiments[35] ibuprofen and naproxen have the same binding site but this question has not been addressed theoretically. In addition, an interesting question emerges is that does curcumin bind to the same position as NSAIDs?

Therefore, in this paper we address the following questions: 1) calculation of the binding free energies of curcumin, ibuprofen and naproxen to monomer Aβ_{1-40} and its mature fibrils using the docking and molecular mechanic-Poisson Boltzmann surface area (MM-PBSA) method; 2) finding binding sites of these ligands and 3) elucidating the role of aromatic rings in ligand binding.

It should be noted that the docking and MD simulation are complementary in solving specific problems of drug design as each of them has its advantages and disadvantages. Docking results provide the information about the location of binding sites and useful insights into the nature of various contributions to the total binding energy but the predictive docking power is limited. MD simulations are computationally more expensive but they are more accurate in the estimation of binding free energies. Therefore we choose both methods for the accurate study of biding affinity of three ligands to monomer and fibrillar structures of Aβ_{1-40}.

In agreement with the experiments[32] we have shown that curcumin binds to Aβ_{1-40} fibrils stronger than NSAIDs. The results obtained for ΔG_{bind} using the MM-PBSA method and Gromos force field 43a1 with explicit water are in accord with experiments.[33,35] Our analysis reveals that in the case of monomer Aβ_{1-40} ibuprofen and naproxen bind to the same position which is different

from the binding site of curcumin. However, for mature fibrils all of three ligands share the same binding site located inside fibrils near loop regions. It is shown that the van der Waals (vdW) interaction between ligand and receptor plays a more important role in binding affinity than the electrostatic one.

MATERIALS AND METHODS

Chemical structures and parametrization of curcumin, ibuprofen and naproxen

The chemical structures of curcumin ($C_{21}H_{20}O_6$), naproxen ($C_{14}H_{14}O_3$) and ibuprofen ($C_{13}H_{18}O_2$) were taken from Pubchem with ID 969516, 156391 and 3672 (http://pubchem.ncbi.nlm.nih.gov). Note that there are R- and S-form of ibuprofen. The latter has been chosen for simulation and will be refereed to as ibuprofen. Two-dimensional plots of three ligands are shown in Figure 1A. We used the PRODRG server[43] to generate their parameters to perform MD simulations with Gromos96 43a1 force field. Names and types of atoms, masses and charges of ligands are shown in Table S1-S3 in Supporting Information (SI).

Crystal structures of monomer Aβ_{1-40}

Since Aβ peptides are highly aggregation-prone in water their monomer structures have not been experimentally resolved yet. In the Protein Data Bank (PDB) two structures with PDB codes 1AML[44] and 1BA4[45] are available for the full-length Aβ_{1-40}. However, these structures are not suitable for aqueous environment as they were obtained in the water-micelle environment with pH$=$ 2.8 and 5.1.[44,45] In order to obtain the structure reliable for docking simulations we have carried out the following simulation. The structure taken from PDB with ID 1BA4 was first heated up to $T = 500$ K using the Gromos96 43a1 force field[46] in explicit water. Then subsequent 5 ns MD simulation was carried at this temperature until the peptide becomes unstructured. A random coil conformation was used as a starting configuration for 300 ns molecular dynamics (MD) simulations at $T = 300$ K. As follow from the time dependence of the C_α root mean square displacement (RMSD) (Fig. S1) the system reaches equilibrium after about 120 ns.

To check if our canonical 300 ns MD simulation generates structures relevant to experimental ones, we calculate chemical shifts δ using snapshots collected during last 180 ns and the SHIFT program.[47,48] Our *in silico* result is in excellent agreement with the NMR experiments of Hou *et al*[49] with correlation level $R = 0.98$ (Fig. S2). The same correlation level has been obtained in 500 ns MD simulation,[50] while Yang and Teplow have reported $R = 0.994$[51] using the replica exchange molecular dynamics (REMD) and recently improved Amber force field PARM99SB.[52] However, the correlation factor of chemical shifts cannot serve as a good indicator of reliability of *in-silico* structural distributions.[50] To understand this problem we calculate the secondary chemical shift defined as $\Delta\delta = \delta - \delta_{\mathrm{RC}}$, where δ_{RC} is a chemical shift for amino acids in random coil state. Using values of NMR δ_{RC} from Wishart *et al*[53] we have the correlation coefficient between the experimental $\Delta\delta_{\mathrm{exp}}$ and our conventional MD (CMD) simulation results $R = 0.42$ (Fig. S2). This correlation level is close to $R = 0.45$ obtained by REMD method[51] (see Fig. S5 in SI of our previous work[50]).

Because, in term of primary and secondary chemical shifts, the quality of structure ensemble obtained by 300 ns CMD is compatible with that of REMD we use the C_α RMSD conformational clustering method[54] implemented in the Gromacs software to screen out dominant structures for studying ligand binding. With the clustering tolerance of 1.0 we have obtained 5 representative structures from snapshots collected in equilibrium during last 180 ns of MD run. We choose a typical structure of the most populated cluster (population is about 84%) as Model 1 (Figure 1) for further docking and MD simulations. Since one structure obtained from 300 ns CMD simulation may not provide unbiased results on binding affinity we will also use structures of three dominant clusters obtained by REMD[51] as receptors. These structures have been provided by Prof. D. Teplow and will be refereed to as Models 2, 3 and 4 (Figure 1). Note that REMD study of $A\beta_{1-40}$ has been also carried by Sgourakis and Garcia[55] but their structures are not available for us.

Solid state NMR structures of $A\beta_{9-40}$ fibrils

Because eight residues of the N-terminus of $A\beta_{1-40}$ are disordered in the fibrillar state,[56] they are neglected in the construction of fibril structures. We perform docking simulation using 2-fold-

symmetric fibrils of six (6Aβ_{9-40}) and twelve (12Aβ_{9-40})[56] peptides and 3-fold symmetric fibrils of nine (9Aβ_{9-40}) and 18 (18Aβ_{9-40})Aβ_{9-40} chains.[57] The corresponding structures were kindly provided by Dr. R. Tycko. Structure of 6Aβ_{9-40} (Figure 1) will be also used for MD simulations in the presence of ligands. Note that experimental structures for 6Aβ_{9-40}-ligand complexes are not available. Therefore initial conformations, used for MD simulation, have been generated by docking ligand to NMR structures of receptor.

Docking method

AutodockTools 1.5.4[58] is used to prepare PDBQT files for the full-length Aβ peptide, fibrils of truncated peptides and three ligands. To dock curcumin, naproxen and ibuprofen to various receptors PDBQT files were used as the input for the Autodock Vina version 1.1[59] which uses the idea of empirical scoring[60,61] that the total binding free energy can be separated into several physically distinct contributions. Autodock Vina is approximately two orders of magnitude faster than Autodock 4.[59] Moreover this method also significantly improves the accuracy of the binding mode prediction compared with Autodock 4.[59]

A modified version of the CHARMM force field was implemented[62,63] to describe atomic interactions. In Autodock Vina the Broyden Fletcher Goldfarb Shanno method[64] is employed for local optimization. To obtain accurate results we set the exhaustiveness of global search between 400 and 4000 depending on systems. The maximum energy difference between the worst and best binding modes was chosen to be 7. Twenty binding modes (20 modes of docking) were generated with random starting positions of the ligand, which has fully flexible torsion degrees of freedom. The receptor flexibility is not allowed in our simulations. The center of grids was placed at the center of mass of the receptor. Grid dimensions were chosen large enough to cover the entire receptor.

MD Simulations

The GROMACS 4.5.5 package[65] was used to run MD simulations with the SPC water model[66] and the Gromos96 43a1 force field.[46] This force field has proved to be useful in studying aggregation of peptides[67,68] and ligand binding affinity.[69] The equations of motion were integrated using

a leap-frog algorithm[70] with a time step of 2 fs. The LINCS algorithm[71] was used to constrain the lengths of all covalent bonds with a relative geometrical tolerance of 10^{-04}. The V-rescale temperature coupling, which uses velocity rescaling with a stochastic term,[72] allows one to couple each system to the heat bath with a relaxation time of 0.1 ps. The Berendsen pressure coupling method[73] was applied to describe the barostat with constant pressure of 1 atm. The vdW forces were calculated with a cutoff of 1.4 nm, and the particle mesh Ewald method[74] was employed to treat the long-range electrostatic interactions. The nonbonded interaction pair list, with a cutoff of 1 nm, was updated every 10 fs.

To probe binding affinity of three compounds to monomer Aβ_{1-40} and fibril 6Aβ_{9-40} the MD simulations have been performed at T =300 K. Cubic boxes have been generated with periodic boundary conditions that contain $\approx$ 2500 and 26000 water molecules for Aβ_{1-40}- and 6Aβ_{9-40}− ligand complexes, respectively. Counter ions Na^+ have been added to neutralize systems.

MM-PBSA Method

The details of MM-PBSA method are given in SI. Overall, in this method the binding free energy of ligand to receptor is defined as follows

$$\Delta G_{\text{bind}} = \Delta E_{\text{elec}} + \Delta E_{\text{vdw}} + \Delta G_{\text{sur}} + \Delta G_{\text{PB}} - T\Delta S, \quad (1)$$

where ΔE_{elec} and ΔE_{vdw} are contributions from electrostatic and vdW interactions, respectively. ΔG_{sur} and ΔG_{PB} are nonpolar and polar solvation energies. The entropic contribution $T\Delta S$ is estimated using the normal mode approximation (SI). In order to calculate ΔG_{bind} the MD simulations have been carried out using the Gromos force field 43a1. The structures of receptor–ligand complex obtained in the best docking mode are used as starting configurations for simulations. For each system 300-500 ns and 20 ns MD trajectories were generated for Aβ_{1-40}- and 6Aβ_{9-40}− ligand complexes, respectively. Snapshots collected in equilibrium are used to compute the binding free energy given by Eq. (1).

Tools and Measures Used in the Structure Analysis

The time dependence of the number of hydrogen bond (HB) and side chain (SC) contacts is monitored. HB is formed if the distance between donor D and acceptor A ≤ 3.5 Å and the D-H-A angle $\geq 135^0$. SC contact is considered as formed if the distance between ligand atom and the center of mass of residue side chain ≤ 6.5 Å. The SC contact map is constructed to study the binding process in detail.

RESULTS AND DISCUSSION

Binding of three ligands to monomer Aβ_{1-40}

Docking results. We first dock three ligands to 4 structures of Aβ_{1-40} (Figure 1) using Autodock Vina version 1.1.[59] The binding energies ΔE_{bind}, obtained in the best mode (lowest values), are averaged over 4 structures and shown in Table 1. Within the error bars the binding energies are the same for three ligand. Thus the docking method is not able to distinguish binding affinities of these ligands to monomer Aβ_{1-40}. However, as evident below, more accurate MD simulations support the superiority of curcumin.

For the model 1 of monomer Aβ_{1-40} curcumin is located near both terminals while naproxen and ibuprofen bind to the same site near the loop containing GLU11 and GLY12 (Figure 2). Interestingly, for models 2, 3 and 4 naproxen and ibuprofen also have the same binding position in the best docking mode (Fig. S3-S5 in SI). The binding position of curcumin in Model 2 is closer to these ligands compared to other models (Figure 2 and Fig. S3-S5). The fact that NSAIDs share the same binding position agrees with the autoradiography and fluorescence experiments by Agdeppa *et al.*[35]

The HB networks between ligands and Aβ_{1-40} (Model 1) in the best docking mode are shown in lower panel of Figure 2. Curcumin has one HB with ASP1 of the receptor, while naproxen and ibuprofen have three HBs with GLU11 and GLY12. Obviously, the HB interaction is not a key factor controlling binding affinity because ibuprofen has ΔE_{bind} higher than curcumin despite the former has more HBs than the latter. Since curcumin, naproxen and ibuprofen have 10, 7 and 6 SC

contacts the SC interaction plays a decisive role in their binding affinity. This conclusion is also valid for Models 2, 3 and 4 of Aβ_{1-40} (results not shown).

Estimation of binding free energies by MM-PBSA method. The docking method is good for predicting a binding position of ligand, but not accurate enough for estimation of binding energies. Therefore, in this section we estimate ΔG_{bind} by the MM-PBSA method.[75,76] The structures of Aβ_{1-40}–ligand complexes obtained in the best docking mode (upper panel of Figure 2 for Model 1 and Figs. S3-S5 for Models 2-4) were used as starting conformations for MD simulations with GROMACS 4.5.5 package.[65] As follows from the time dependence of the interaction energy between receptor and ligand the systems reach equilibrium at different time scales marked by arrows (Fig. S6-S9). For Model 1, 3 and 4 (Fig. S6, S8, and S9) the equilibration time of Aβ_{1-40}–curcumin complex is larger than complexes with naproxen and ibuprofen. This is presumably because curcumin is bigger leading to more complex interactions with the receptor. The situation becomes different for Model 2 where the complex with curcumin gets equilibrated even faster than naproxen and ibuprofen (Fig. S7) suggesting that the equilibration time depends not only on ligand structure but also on topological and chemical properties of the binding site.

As shown below, within the same Gromos force field the time scale to reach equilibrium for complex of fibril 6Aβ_{9-40} and ligand is about one order of magnitude shorter than Aβ_{1-40}. This is because Aβ_{1-40} lacks a well-defined binding site (Figure 2, Figs. S3-S5), while a ligand moves within the binding pocket of 6Aβ_{9-40}. For other systems with well-defined binding pocket the relaxation time is of $\approx$ 10 ns.[69]

Snapshots collected every 100 ps in equilibrium were used to estimate ΔG_{bind} by the MM-PBSA protocol (Eq. (1) and SI). The results that have been averaged over four models are shown in Table 2. For curcumin the vdW contribution dominates over the electrostatic interaction, but for naproxen and ibuprofen the Coulomb contribution is larger in magnitude than the vdW term. ΔE_{elec} is positive for NSAIDs because these ligands have charge of -1 while the total charge of Aβ_{1-40} is -3. The charge of naproxen and ibuprofen is non-zero due to the carboxyl group that becomes carboxylate group in the aqueous environment. Having total zero charge curcumin dis-

plays attractive Coulomb interaction with the receptor (Table 2). Note that the contribution of electrostatic interactions is largely compensated by the polarization term $\Delta G_{\rm PB}$.

In the harmonic approximation the solute entropy contribution is nearly the same for naproxen and ibuprofen complexes, but two-fold smaller than curcumin (Table 2). This is because curcumin has 21 carbon atoms, while naproxen and ibuprofen have 14 and 13 carbon atoms only. For this very reason the nonpolar term $\Delta G_{\rm sur}$ of NSAIDs is also twice smaller than curcumin.

Curcumin and naproxen show very strong binding affinity to monomer Aβ_{1-40} having $\Delta G_{\rm bind} = -19.1 \pm 6.4$ and -8.7 $\pm$ 2.4 kcal/mol, respectively (Table 2). Within the error bars these estimations are close to the experimental values obtained for fibrillar structures.[33,35] Much weaker binding affinity was observed for ibuprofen with $\Delta G_{\rm bind} \approx$ -3.2 kcal/mol which is higher the experimental result -6.8 kcal/mol measured for fibrils (Table 2). MM-PBSA calculations give the following ranking for binding affinity to monomer Aβ_{1-40}:

$$ibuprofen \rightarrow naproxen \rightarrow curcumin, \qquad (2)$$

where the ascending ordering is used. As will shown below, this ranking also holds for ligand binding to fibrils.

Role of aromatic rings in binding affinity of ligands to Aβ_{1-40}. Since the vdW interaction dominates over the electrostatic interaction in binding affinity we consider the contribution of individual atoms of ligand to the vdW interaction energy. Curcumin, naproxen and ibuprofen, respectively, have 35, 23 and 19 atoms that are numbered as shown in Fig. S10. Using the Gromacs software we have calculated the vdW interaction energy of each atom with receptor in equilibrium (only snapshots collected after arrows in Fig. S4-S7 are used for calculation) and the results have been averaged over four models. Curcumin has 4 key atoms (9, 11, 18 and 26) that have vdW interaction energy $E_{\rm vdW} < -2$ kcal/mol (Figure 3) but three of them belong to aromatic rings. However, contributions from aromatic ring atoms are not homogeneous leading to their total contribution of about 51.4%. Thus, aromatic rings of curcumin do not dominate over other parts in vdW interac-

tion with monomer Aβ_{1-40} although they have three key residues.

Similar to curcumin the aromatic ring of ibuprofen, which involves 10 atoms, has almost the same contribution to E_{vdW} (46,7%) as other fragments. Among 9 key atoms (5, 7, 9, 11, 13, and 16-19) which have $E_{\mathrm{vdW}} < -1$ kcal/mol (Figure 3) one has four atoms 7, 9, 11 and 13 from the aromatic ring.

The situation becomes different in the case of naproxen (Figure 3), where aromatic rings dominate over other parts as their contribution is 71.1%. Five (atoms 10, 12, 20 and 22) of 7 key atoms with $E_{\mathrm{vdW}} < -1.5$ kcal/mol belong to aromatic rings.

Hydrogen bonding and side chain interaction of curcumin are stronger than naproxen and ibuprofen. Since qualitative results are the same for four models of monomer Aβ_{1-40} we will focus on the Model 1. In order to better understand the nature of binding of three ligands we monitor the time dependence of HBs between receptor and ligand (Figure 4). Having calculated the time average of the number of HBs in equilibrium we obtain $\overline{HB(t)} = 2.34$, 0.27 and 0.07 for curcumin, naproxen and ibuprofen, respectively. Thus, contrary to the docking result (Figure 2), curcumin has more HBs than NSAIDs and the binding ranking (Eq. (2)) is consistent with our MD results on HB networks.

Figure 5 shows the probability of occurrence of HB between ligand and a given residue of receptor. This quantity is defined as the number of HB formation times divided by the total number of recorded snapshots. Curcumin prefers to form HBs with both terminals with very strong binding to residue GLY-38, while NSAIDs have more HBs with the region 10-16 (Figure 5). The HB network of curcumin with monomer Aβ_{1-40} is much stronger than naproxen and ibuprofen. This is in accord with the estimations of ΔG_{bind} (Table 2).

Fig. S11 shows time dependence of SC contacts between Aβ_{1-40}-Model 1 and three ligands. The average numbers of SC contacts, obtained in equilibrium for curcumin, naproxen and ibuprofen (Fig. S11) indicate that together with hydrogen bonding the side chain interaction plays an important role in ligand association. In order to get a more detailed picture on binding we have constructed SC contact map (Fig. S12) which shows the probability of occurrence of contacts

between each atom of ligand and the SC of receptor amino acids. In agreement with the HB picture (Figure 5) curcumin spends more time near two ends of Aβ_{1-40} than other regions, frequently binding to residue GLY-37 and GLY-38. Naproxen has less SC contacts compared to curcumin displaying strong binding to PHE-20. Contrary to curcumin and naproxen, ibuprofen does not bind to specific residues (Fig. S12) and this is a reason why ibuprofen has the lowest SC interaction and binding affinity. Comparing Figure 5 and Fig. S12 one can see that both HB and SC data support the binding ranking given by Eq. (2).

Binding site predicted by the docking method for curcumin is the most probable. Since monomer Aβ_{1-40} is almost unstructured and does not have a well-defined binding pocket it is interesting to know if the binding site predicted by the docking method (Figure 2) remains the most probable in MD runs. We will consider Model 1 because similar results have been also obtained for three remaining models. Starting from the conformation obtained in the best docking mode during 300 ns simulations curcumin may run away from the binding location but revisits it again and again (Movie S1 in SI). Naproxen and ibuprofen spend less time around their binding sites obtained by docking than curcumin (Movies S2 and S3 in SI). In order to demonstrate this clearly we plot data shown in Fig. S12 in a different way (Figure 6). In Figure 6 the probability of formation of SC contacts between ligand and receptor is defined in such a way that a contact is considered as formed if the distance between any ligand atom and the center of mass of residue < 6.5 Å. Symbol X refers to those residues that have SC contacts with ligand in the best docking mode conformation. Clearly, residues of the binding site predicted by the docking method for curcumin are the most visited by ligand during MD simulation. However this does not hold for NSAIDs. Naproxen binds to PHE20 (51.8%) and VAL36 (54%) very often but these residues do not belong to the binding site followed from the docking calculation (Figure 6). Ibuprofen displays the binding propensity to residues HIS6 (15.4%), TYR10 (17.9%), HIS13 (16.2%), GLN12 (18.1%), VAL18 (16.2%) and GLY25 (16.5%) higher than to others but only TYR10, HIS13 and GLN15 belong to the docking binding region. Nevertheless, naproxen and ibuprofen have the tendency to bind to the same place (Figure 6).

Binding to two-fold symmetric fibril 6Aβ_{9-40}

The results obtained for monomer Aβ_{1-40} by MD simulations indicate that curcumin is the most prominent ligand. However, they can not be directly compared with the experiments[32,33,35] which have been carried out on mature fibrils. Recall that it is very difficult to perform experiments for Aβ monomer in water as it has high propensity to aggregation. Therefore, to make the direct comparison of theoretical results with the experiments one should consider fibril structures. Here we consider 6Aβ_{9-40} system but more complex structures will be discussed with the help of the docking method in the next section.

Docking results. Binding positions in the best mode obtained by the Autodock Vina version 1.1 are shown in Figure 7. In difference from the monomer case (Figure 2), all of three ligands have the same binding site inside the upper patch of three β-hairpins. The corresponding binding energies of ligands to 6Aβ_{9-40} are listed in Table 1. In agreement with the experiments[32,33,35] and results obtained by the MM-PBSA method for monomer (Eq. (2)), curcumin at least marginally dominates over NSAIDs having $\Delta E_{\rm bind} = -7.0$ kcal/mol that is lower than $\Delta E_{\rm bind} = -6.7$ and -6.0 kcal/mol for naproxen and ibuprofen, respectively.

Curcumin forms 3 HBs with the receptor including two with LYS28 and one with SER26 from peptide III (lower panel of Figure 7). Naproxen has 2 HBs with LYS28(I) and PHE20 (III), while ibuprofen has only one HB with LYS28(II). Thus based on the HB networks one can explain the ranking of binding affinity in Eq. (2) that the lower is $\Delta E_{\rm bind}$ the larger is the number of HBs.

Binding free energy: MM-PBSA results. The conformations obtained by the docking method (Figure 7), are used as starting configurations for 20 ns MD simulations. The systems reach equilibrium at time scales of ≈ 10 ns (Fig. S13) that are much shorter than the monomer case (Fig. S6-S9). This is because ligands have the binding pocket inside fibrils and they stay there during the whole MD run (Movies 4, 5 and 6 in SI). Snapshots collected in equilibrium, i.e. after times marked by arrows in Fig. S13 are used for estimating the binding free energy by MM-PBSA method[75,76] (Table 2). For curcumin we have $\Delta G_{\rm bind} =$ -13.5 kcal/mol which is in excellent agreement with the experimental value of -13.33 kcal/mol.[33] Thus both experiment and simulation indicate that cur-

cumin has very strong binding affinity with the inhibition constant IC50 $\sim$ nM. For naproxen, the agreement between theory and experiment is not as good as curcumin but the simulation correctly captures the experimental range of IC50 $\sim \mu$M.[35] For ibuprofen the MM-PBSA method provides $\Delta G_{\rm bind} = -8.31$ kcal/mol that is lower than the experimental value -6.8 kcal/mol (Table 2). Given that this approach involves a number of approximations our simulation results should be considered as reasonable.

Nature of ligand binding to 6Aβ_{9-40}. The time dependence of the number of HBs between ligand and receptor is shown in Figure 8. Their time average value estimated in equilibrium $\overline{HB(t)} =$ 2.19, 0.56, and 1.21 for curcumin, naproxen and ibuprofen, respectively. The strong HB interaction between curcumin and 6Aβ_{9-40} causes its high binding affinity. However, this scenario is not valid if one compares naproxen with ibuprofen as the latter has more HBs but the binding is less tight. To shed more light on their binding nature we calculate SC contacts (Fig. S14). In equilibrium one has the average number of SC contacts $\overline{SC(t)} = 25.17$, 18.16 and 17.06 for curcumin, naproxen and ibuprofen, respectively. Therefore, the fact that the binding of ibuprofen is weaker than naproxen is caused by the smaller number of SC contacts or weaker side chain interaction.

As in the monomer Aβ_{1-40} case, the electrostatic interaction between curcumin and 6Aβ_{9-40} is attractive while it becomes repulsive for NSAIDs due to difference in charges of ligands (Table 2). The nonpolar solvation energy $\Delta G_{\rm sur}$ is smaller compared to the monomer case as the solvent-accessible surface area A (see SI) is larger in the presence of more peptides. $\Delta G_{\rm sur}$ of curcumin is lower because its size is bigger than others. For all of ligands the vdW interaction dominates over the combined contribution of electrostatic and polar terms playing the decisive role in binding affinity to 6Aβ_{9-40}.

Fig. S15 shows the contributions of ligand individual atoms to the the vdW interaction with receptor. The results have been obtained in equilibrium MD simulations. For curcumin atoms 3, 4, 6, 9, 11, 13, 23, 24, 26, 28, 30 and 33 of aromatic rings and atoms 1, 2, 7, 31, 34 and 35 from other fragments are important for both monomer and fibril (compare Figure 3 and Fig. S15). A difference is seen for carbon atom 20 which has slightly positive contribution in the fibril case. The

role of individual atoms is also almost the same for monomer and fibril complexes with naproxen and ibuprofen (Figure 3 and Fig. S15). However, atoms 1 and 3 of ibuprofen have negative and positive contribution for monomer (Figure 3) and fibril (Fig. S15), respectively.

Overall, as in the monomer Aβ_{1-40} case aromatic rings of naproxen dominate over the remaining parts while for curcimin and ibuprofen they have the same contribution to the vdW interaction energy as other fragments. One can show that the contribution from aromatic ring atoms is 52.7, 70.4 and 49.2% for curcumin, naproxen and ibuprofen, respectively. These percentages are very close to those of the monomer case.

Binding to more complex Aβ fibril structures

The results, obtained for binding affinity of ligands to the fibril structure 6Aβ_{9-40} and monomer Aβ_{1-40}, unambiguously support domination of curcumin over naproxen and ibuprofen in binding affinity, but it remains unclear if this does hold for more complex fibril structures. In this section we restrict ourselves to study of 2-fold symmetric 12Aβ_{9-40}, and 3-fold symmetric 9Aβ_{9-40}, and 18Aβ_{9-40} fibrils using AutodockTools 1.5.4.[58]

Binding to 3-fold symmetric 9Aβ_{9-40}. For docking we use the structure, resolved by Paravastu et al.[57] The lowest energy conformations of the receptor with three ligands are shown in Figure 9. Similar to the 6Aβ_{9-40} case (Figure 7) all of ligands bind to the same place inside the patch of three peptides. The binding energies ΔE_{bind} =-8.8, -7.9 and 7.5 kcal/mol for curcumin, naproxen and ibuprofen, respectively. Thus, as in the monomer and 6Aβ_{9-40} cases the binding affinity of curcumin is the highest and one can expect that this ligand is the most efficient in degradation of 9Aβ_{1-40} aggregates.

Although curcumin displays the highest propensity to binding, its HB network the weakest one. It has only one HB with PHE108 (I) of 9Aβ_{9-40}, while naproxen forms two HBs with LYS148 (II) and ILE151 (II). Ibuprofen even has three HBs with LYS148 (II) and ILE151 (II) (Figure 9). Therefore, HB network itself does not control binding affinity of these ligands. The high binding of curcumin comes from the strong SC interaction having 21 SC contacts that are much more than 13 and 16 SC contacts of naproxen and ibuprofen. However the situation remains ambiguous for

NSAIDs because the binding energy of naproxen is lower than ibuprofen despite naproxen has less HB as well as SC contacts. The solution of this issue requires further investigation but one can believe that the binding ranking (Eq. (2)) predicted by the docking method remains valid for three-fold symmetric 9Aβ_{9-40} fibril for the following reason. According to our recent study (MH Viet and MS Li, unpublished results), the higher is binding affinity to Aβ fibrils the larger is the total number of carbon atoms of ligand. Because naproxen has more carbon atoms than ibuprofen one can expect that the former has higher binding affinity.

Binding to 2-fold symmetric 12Aβ_{9-40} and 3-fold symmetric 18Aβ_{9-40}.

We now consider larger targets of 12 and 18 Aβ_{9-40} peptides. The binding energies obtained by the docking method are listed on Table 1. Clearly for both targets, in accord with the experiments,[32] curcurin remains the best binder with the ranking given by Eq. (2). In the best binding mode curcumin, naproxen and ibuprofen have 2, 3 and 0 HBs with receptor 12Aβ_{9-40}, respectively (Fig. S16). The strong binding of curcumin with ΔE_{bind} =-8.6 kcal/mol comes from strong SC interaction having 24 side chains contacts. NSAIDs have lower binding affinity (ΔE_{bind} =-7.7, and -6.9 kcal/mol for naproxen and ibuprofen) because they have less SC contacts (18 and 20 SC contacts for naproxen and ibuprofen). The lower binding of ibuprofen compared to naproxen is probably due to the weaker HB network and smaller number of carbon atoms.

For the three-fold symmetric 18Aβ_{9-40} (Fig. S17), we have the same binding ranking (Eq. (2)) with ΔE_{bind} =-9.5, -9.1 and -8.3 kcal/mol for curcumin, naproxen and ibuprofen. Curcumin has no HB contact with the receptor, whereas naproxen and ibuprofen have 2 and 3 HBs. Therefore, hydrogen bonding is not responsible for its strong binding affinity. One can show that SC interaction plays a decisive role because 18Aβ_{9-40} has 31 SC contacts with curcumin. This number of contacts is markedly larger than 21 and 18 contacts for naproxen and ibuprofen. Thus, the binding nature is defined by the SC interaction.

It should be noted that, in agreement with the experiment,[35] NSAIDs have the same binding site (Fig. S16) near the loop region inside the upper 6-peptide patch of 12Aβ_{9-40}. Curcumin also docks near the loop region but inside the lower patch. However, due to structure symmetry one

may observe the same binding site for three ligands on experiments. For 18Aβ_{9-40} curcumin and NSAIDs are located at the same position near loops (Fig. S17) where they can have more contacts with the receptor than other places.

Binding to fibril 5Aβ_{17-42}

Using the docking method we have also calculated the binding energy of three ligands to fibril of five truncated peptides 5Aβ_{17-42} (PDB ID: 2BEG[12]). In the best mode the they have the same binding site inside the fibril (Fig. S18). The binding energy ΔE_{bind} = -7.5, -6.8 and -6.8 kcal/mol for curcumin, naproxen and ibuprofen, respectively, suggesting that curcumin also binds to Aβ_{1-42} aggregates more tightly than NSAIDs.

Binding in low pH and hexafluoroisopropanol/water environment

At pH= 2.8 and 5.1 monomer Aβ_{1-40} adopts the helix-rich structure with PBD ID 1AML[44] and 1BA4[45] (Fig. S19). In the best docking mode, for pH=2.8 (5.1) one has ΔE_{bind} =-5.7 (-6.3), -5.4 (-5.7), and -5.1 (-5.1) kcal/mol for curcumin, naproxen and ibuprofen, respectively. The values in parentheses are for pH=5.1. Therefore, NSAIDs also show the lower binding affinity than curcumin at low pH.

Upon addition of a certain amount of hexafluoroisopropanol (HFIP) to water Aβ_{1-42} becomes structured and the corresponding structure has been solved by Tomaselli *et al*[77] (PDB ID: 1Z0Q). Using this structure and the docking method we obtain ΔE_{bind} = -5.8, -5.4 and -4.8 kcal/mol for curcumin, naproxen and ibuprofen (Fig. S20). This result implies that the ranking of binding affinity given by Eq. (2) remains valid for Aβ_{1-42} in the HFIP/water environment.

Conclusion

1. The effect of naproxen and ibuprofen on degradation of Aβ fibrils has been studied by Klimov *et al*[39–42] but they have focused on the multi-ligand collective dynamics. In contrast, our study concerns pharmaceutical aspects of this problem calculating the binding free energies that can be directly compared with experimental results on inhibition constants. Our

estimates of ΔG_{bind} (Table 2) are in good agreement with experiments [33,35] showing that curcumin is the most potent ligand.[32] Our study also reveals that curcumin and naproxen may be used as a drug to interfere Aβ fibrillogenesis but not ibuprofen. Thus, naproxen is not only a non-steroidal anti-inflammatory drug but also as a good inhibitor for Aβ aggregation having IC50 in the range of 10 nM.

2. Based on the results obtained by the docking and MD simulations we predict that curcumin has the same binding pocket as NSAIDs inside Aβ fibrils. It would be interesting to check validity of this prediction for other ligands.

3. The vdW interaction is found to dominate over the electrostatic interaction in binding affinity. The detailed analysis about contributions of individual ligand atoms to the vdW interaction energy shows that aromatic rings of curcumin and ibuprofen have almost the same contribution as remaining parts, while they dominate in the case of naproxen. This conclusion holds for both monomer and fibril cases.

4. It is well known that curcumin strongly interferes with Aβ aggregation. On the other hand, as follows from our and experimental study it can tightly binds to fibrils. This suggests that inhibition of fibril formation is via the binding mechanism. Namely, curcumin binds to Aβ fibrils modulating their propensity to aggregation. Such a mechanism has been observed for other systems.[50,78]

5. The fact that NSAIDs also show the lower binding affinity than curcumin is presumably valid at low pH and HFIP/water environment. However this result has been obtained by the docking method its validity should be checked by more sophisticated methods.

Acknowledgments

We benefit a lot from useful discussions with G. M. Cole, Binh Khanh Mai and Man Hoang Viet. We are very thankful to M. G. Zagorski for providing experimental results on chemical shifts, Prof. R. Tycko for solid state NMR structures of Aβ fibrils, and D. B. Teplow and M. Yang for

sharing their REMD data on structures of the most populated clusters of monomer systems. The financial support from Narodowe Centrum Nauki in Poland (grant No 2011/01/B/NZ1/01622) and Department of Science and Technology at Ho Chi Minh city, Vietnam, and allocation of CPU time at the Supercomputer Center TASK in Gdansk (Poland) are highly appreciated.

Supporting Information Available: MM-PBSA method, Supplementary Figures S1-20 and Movie S1-S6. This material is available free of charge via the Internet at http://pubs.acs.org.

References

(1) Henderson, A. S.; Jorm, A. F. *Dementia*; John Wiley & Sons Ltd, 2002; Chapter 1.

(2) Greene, J. D. W.; Baddeley, A. D.; Hodges, J. R. *Neuropsychologia* **1996**, *34*, 537–551.

(3) Price, B. H.; Gurvit, H.; Weintraub, S.; Geula, C.; Leimkuhler, E.; Mesulam, M. *Arch. Neuro.* **1993**, *50*, 931–937.

(4) Esteban-Santillan, C.; Praditsuwan, R.; Ueda, H.; Geldmacher, D. S. *J. Am. Geriatr. Soc.* **1998**, *46*, 1266–1269.

(5) Hardy, J.; Selkoe, D. J. *Science* **2002**, *297*, 353–356.

(6) Alonso, A.; Zaidi, T.; Novak, M.; Grundke-Iqbal, I.; Iqbal, K. *Proc. Natl. Acad. Sci.* **2001**, *98*, 6923–6928.

(7) Citron, M. *Nat. Rev. Neurosci.* **2004**, *5*, 677–685.

(8) Aguzzi, A.; O'Connor, T. *Nat. Rev. Dru.* **2010**, *9*, 237–248.

(9) Eanes, E. D.; Glenner, G. G. *J. Histochem. Cytochem.* **1968**, *16*, 673–677.

(10) Kirschner, D. A.; Abraham, C.; Selkoe, D. J. *Proc. Natl. Acad. Sci. USA* **1986**, *83*, 503–507.

(11) Petkova, A. T.; Ishii, Y.; Balbach, J.; Antzutkin, O.; Leapman, R.; Delaglio, F.; Tycko, R. *Proc. Natl. Acad. Sci. USA* **2002**, *99*, 16742–16747.

(12) Luhrs, T.; Ritter, C.; Adrian, M.; Riek-Loher, D.; Bohrmann, B.; Doeli, H.; Schubert, D.; Riek, R. *Proc. Natl. Acad. Sci. USA* **2005**, *102*, 17342–17347.

(13) Kayed, R.; Head, E.; Thompson, J. L.; McIntire, T. M.; Milton, S. C.; Cotman, C. W.; Glabe, C. G. *Science* **2003**, *300*, 486–489.

(14) Caughey, B.; Lansbury, P. T. *Annu. Rev. Neurosci.* **2003**, *26*, 267–298.

(15) Cummings, J. L. *N. Engl J. of Med.* **2004**, *351*, 56–67.

(16) Yatin, S. M.; Yatin, M.; S., V.; B., A. K.; A., B. D. *J. Neurosci Res.* **2001**, *63*, 395–401.

(17) Dolphin, G. T.; Chierici, S.; Ouberai, M.; Dumy, P.; Garcia, J. *Chembiochem* **2008**, *9*, 952–963.

(18) Bush, A. I. *Neurobiol. Aging* **2002**, *23*, 1031–1038.

(19) Evans, C. G.; Wisen, S.; Gestwicki, J. E. *J. Biol. Chem.* **2006**, *281*, 33182–33191.

(20) Svennerholm, L. *Life Sci.* **1994**, *55*, 2125–2134.

(21) Castillo, G. M.; Ngo, C.; Cummings, J.; Wight, T. N.; Snow, A. D. *J. Neurochem.* **1997**, *69*, 2452–2465.

(22) Nitz, M.; Fenili, D.; Darabie, A.; Wu, L.; Cousins, J.; McLaurin, J. *FEBS J.* **2008**, *275*, 1663–1674.

(23) Tjerngber, L. O.; Naslund, J.; Lindqvist, F.; Jahannson, J.; Karlstrom, A. R.; Thyberg, J.; Terenius, L.; Nordstedt, C. *J. Biol. Chem.* **1996**, *271*, 8545–8548.

(24) Soto, C. M.; Kindy, S.; Baumann, M.; Frangione, B. *Biochem. Biophys. Res. Co.* **1996**, *226*, 672–680.

(25) Adessi, C.; Soto, C. *Drug Dev. Res.* **2002**, *56*, 184–193.

(26) Li, H. Y.; Monien, M. B.; Lomakin, A.; Zemel, R.; Fradinger, E. A.; Tan, M. A.; Spring, S. M.; Urbanc, B.; Xie, C. W.; Benedek, G. B.; Bitan, G. *Biochemistry* **2010**, *49*, 6358–6364.

(27) Wu, C.; Murray, M. M.; Summer, S. L. B. L.; Condron, M. M.; Bitan, G.; Shea, J. E.; Bowers, M. T. *J. Mol. Biol.* **2009**, *387*, 492–501.

(28) Takahashi, T.; Tada, K.; Mihara, H. *Mol. Biosyst.* **2009**, *5*, 986–991.

(29) Hawkes, C. A.; Ng, V.; MacLaurin, J. *Drug Dev. Res.* **2009**, *70*, 111–124.

(30) Yamin, G.; Ono, K.; Inayathullah, M.; Teplow, D. B. *Curr. Phar. Design* **2008**, *14*, 3231–3246.

(31) Oken, B. S.; Storzbach, D. M.; Kaye, J. A. *Arch Neurol.* **1998**, *55*, 1409–1415.

(32) Yang, F. S.; Lim, G. P.; Begum, A. N.; Ubeda, O. J.; Simmons, M. R.; Ambegaokar, S. S.; Chen, P. P.; Kayed, R.; Glabe, C. G.; Frautschy, S. A.; Cole, G. M. *J. Biol. Chem.* **2005**, *280*, 5892–5901.

(33) Ryu, E. K.; Choe, Y. S.; Lee, K. H.; Choi, Y.; Kim), B. T. *J. Med. Chem.* **2006**, *49*, 6111–6119.

(34) Ringman, J. M.; Frautschy, S. A.; Cole, G. M.; Masterman, D. L.; Cummings, J. L. *Current Alzheimer's Res.* **2005**, *9*, 131–136.

(35) Agdeppa, E. D.; Kepe, V.; Petric, A.; Satyamurthy, N.; Liu, J.; Huang, S. C.; Small, G. W.; Coled, G. M.; Barrio, J. R. *Neuroscience* **2003**, *117*, 723–730.

(36) Vlad, S. C.; Miller, D. R.; Kowall, N. W.; Felson, D. T. *Neurology* **2008**, *70*, 1672–1677.

(37) Imbimbo, B. *Expert Opin Investig Drug* **2009**, *18*, 1147–1168.

(38) Cole, G. M.; Frautschy, S. A. *CNS Neuro Disord Drug Targets* **2010**, *9*, 140–148.

(39) Raman, E. P.; Takeda, T.; Klimov, D. K. *Biophys. J.* **2009**, *97*, 2070–2079.

(40) Takeda, T.; Kumar, R.; Raman, E. P.; Klimov, D. K. *J. Phys. Chem. B* **2010**, *114*, 15394–15402.

(41) Takeda, T.; Chang, W. L. E.; Raman, E. P.; Klimov, D. K. *Proteins* **2010**, *78*, 2849–2860.

(42) Kim, S.; Chang, W. E.; Kumar, R.; Klimov, D. K. *Biophys. J* **2011**, *100*, 2024–2032.

(43) Schuttelkopf, A. W.; van Aalten, D. M. F. *Acta Crystallogr.* **2004**, *D60*, 1355–1363.

(44) Sticht, H.; Bayer, P.; Willbold, D.; Dames, S.; Hilbich, C.; Beyreuther, K.; Frank, R. W.; Rosch, P. *Eur. J. Biochem.* **1995**, *233*, 293–298.

(45) Coles, M.; Bicknell, W.; Watson, A. A.; Fairlie, D. P.; Craik, D. J. *Biochemistry* **1998**, *37*, 11064–11077.

(46) van Gunsteren, W.; Billeter, S. R.; Eising, A. A.; Hünenberger, P. H.; Krüger, P.; Mark, A. E.; Scott, W.; Tironi, I. *Biomolecular Simulation: The GROMOS96 Manual and User Guide.*; Vdf Hochschulverlag AG an der ETH: Zurich, 1996.

(47) Xu, X. P.; Case, D. A. *J. Biomol. NMR.* **2001**, *21*, 321–333.

(48) Xu, X. P.; Case, D. A. *Biopolymers* **2002**, *65*, 408–423.

(49) Hou, L.; Shao, H.; Zhang, Y.; Li, H.; Menon, N. K.; Neuhaus, E. B.; Brewer, J. M.; Byeon, I.-J. L.; Ray, D. G.; Vitek, M. P.; Iwashita, T.; Makula, R. A.; Przybyla, A. B.; Zagorski, M. G. *J. Am. Chem. Soc* **2004**, *126*, 1992–2005.

(50) Viet, M. H.; Li, M. S. *J. Chem. Phys.* **2012**, *136*, 245105.

(51) Yang, M.; Teplow, D. B. *J. Mol. Biol.* **2008**, *384*, 450–464.

(52) Hornak, V.; Abel, R.; Okur, A.; Strockbine, B.; Roitberg, A.; Simmerling, C. *Proteins* **2006**, *65*, 712–725.

(53) Wishart, D. S.; Bigam, C. G.; Holm, A.; Hodges, R. S.; Sykes, B. D. *J. Biomolecular NMR* **1995**, *5*, 67–81.

(54) Daura, X.; Gademann, K.; Jaun, B.; Seebach, D.; van Gunsteren, W.; Mark, A. *Angew. Chem. Int. Ed.* **1999**, *38*, 236–240.

(55) Sgourakis, N. G.; Yan, Y. L.; McCallum, S. A.; Wang, C. Y.; Garcia, A. E. *J. Mol. Biol* **2007**, *368*, 1448–1457.

(56) Petkova, A. T.; Yau, W. M.; Tycko, R. *Biochemistry* **2006**, *45*, 498–512.

(57) Paravastu, A. K.; Leapman, R. D.; Yau, W. M.; Tycko, R. *Proc. Natl. Acad. Sci. (USA)* **2008**, *105*, 18349–18354.

(58) Sanner, M. F. *J. Mol. Graphics Mod.* **1999**, *17*, 57–61.

(59) Trott, O.; Olson, A. J. *J. Comput. Chem.* **2010**, *31*, 455–461.

(60) Bohm, H. *J. Comput. Aided Mol. Design* **1994**, *8*, 243–256.

(61) Mihajlovic, M.; Mitrasinovic, P. *Molecular Simulation* **2009**, *35*, 311–324.

(62) Morris, G. M.; Godsell, D. S.; Halliday, R. S.; Huey, R.; Hart, W. E.; Belew, R. K.; Olson, A. J. *J. Comput. Chem.* **1998**, *19*, 1639–1662.

(63) Morris, G. M.; Goodsell, D. S.; Huey, R.; Olson, A. J. *J. Comput-Aided. Mol. Des.* **1996**, *10*, 293–304.

(64) Shanno, D. F. *Matthematics of Computation* **1970**, *24*, 647–656.

(65) Hess, B.; Kutzner, C.; van der Spoel, D.; Lindahl, E. *J. Chem. Theory Comput.* **2008**, *4*, 435–447.

(66) Berendsen, H. J. C.; Postma, J.; van Gunsteren, W.; Hermans, J. *Intermolecular Forces*; Reidel: Dortrecht, 1996.

(67) Nguyen, P. H.; Li, M. S.; Stock, G.; Straub, J. E.; Thirumalai, D. *Proc. Natl. Acad. Sci. (USA)* **2007**, *104*, 111–116.

(68) Nam, H. B.; Kouza, M.; Zung, H.; Li, M. S. *J. Chem. Phys.* **2010**, *132*, 165104.

(69) Nguyen, T. T.; Mai, B. K.; Li, M. S. *J. Chem. Info. Model.* **2011**, *51*, 2266–2276.

(70) Hockney, R. W.; Goel, S. P.; Eastwood, J. *J. Comp. Phys.* **1974**, *14*, 148–158.

(71) Hess, B.; Bekker, H.; Berendsen, H. J. C.; Fraaije, J. G. E. M. *J. Comp. Chem.* **1997**, *18*, 1463–1472.

(72) Bussi, G.; Donadio, D.; Parrinello, M. *J. Chem. Phys.* **2007**, *126*, 014101.

(73) Berendsen, H. J. C.; Postma, J. P. M.; Vangunsteren, W. F.; Dinola, A.; Haak, J. R. *J. Chem. Phys.* **1984**, *81*, 3684–3690.

(74) Darden, T.; York, D.; Pedersen, L. *J. Chem. Phys.* **1993**, *98*, 10089–10092.

(75) Srinivasan, J.; III, T. C.; Cieplak, P.; Kollman, P.; Case., D. *J. Am. Chem. Soc.* **1998**, *120*, 9401–9409.

(76) Kollman, P.; Massova, I.; Reyes, C.; Kuhn, B.; Huo, S.; Chong, L.; Lee, M.; Lee, T.; Duan, Y.; Wang, W.; Donini, O.; Cieplak, P.; Srinivasan, J.; Case, D.; T.E. Cheatham, I. *Acc. Chem. Res.* **2000**, *33*, 889–897.

(77) Tomaselli, S.; Esposito, V.; Vangone, P.; van Nuland, N. A.; Bonvin, A. M.; Guerrini, R.; Tancredi, T.; Temussi, P. A.; Picone, D. *ChemBiochem* **2006**, *7*, 257–267.

(78) Yan, Y. L.; Wang, C. Y. *J. Mol. Biol* **2007**, *369*, 909–916.

Table 1: Shown are binding energies ΔE_{bind} (in kcal/mol) of curcumin, naproxen, and ibuprofen to monomer Aβ_{1-40} and mature fibrils. Results have been obtained in the best mode by the docking method. For Aβ_{1-40} error bars come from averaging over 4 Models.

	Aβ_{1-40}	2-fold 6Aβ_{9-40}	2-fold 12Aβ_{9-40}	3-fold 9Aβ_{9-40}	3-fold 18Aβ_{9-40}
Curcumin	-5.4±0.5	-7.0	-8.6	-8.8	-9.5
Naproxen	-5.3±0.4	-6.7	-7.7	-7.9	-9.1
Ibuprofen	-4.9±0.3	-6.0	-6.9	-7.5	-8.3

Table 2: Binding free energies ΔG_{bind} (kcal/mol) of three inhibitors to monomer Aβ_{1-40} and 2-fold symmetric 6Aβ_{9-40} fibril obtained by the MM-PBSA method. For Aβ_{1-40} error bars come from averaging over 4 Models. The experimental values of ΔG_{bind} are estimated from the inhibition constants K_{i} using the formula $\Delta G_{\text{bind}} = RT\ln(K_{\text{i}})$. Here $R = 1.987 \times 10^{-3}$ kcal/mol, $T = 300$ K, and K_{i} is measured in M. K_i of curcumin and NSAIDs was taken from Ryu *et al*[33] and Agdeppa *et al*,[35] respectively.

		ΔE_{elec}	ΔE_{vdw}	ΔG_{sur}	ΔG_{PB}	$-T\Delta S$	ΔG_{bind}	$\Delta G_{\text{bind}}^{\text{exp}}$
Curcumin	Aβ_{1-40}	-28.5±6.5	-46.2±6.7	-5.2±0.5	37.3±4.1	23.5±0.6	-19.1±6.4	
	6Aβ_{9-40}	-21.99	-49.96	-6.30	39.31	25.44	-13.50	-13.33
Naproxen	Aβ_{1-40}	43.7±8.4	-23.4±4.4	-3.0±0.4	-34.5±11.0	8.3±0.5	-8.7±2.4	
	6Aβ_{9-40}	52.40	-31.73	-4.18	-36.57	10.46	-9.45	-11.33
Ibuprofen	Aβ_{1-40}	45.9±5.3	-14.4±2.5	-2.2±0.4	-40.2±5.3	7.7±1.0	-3.2±2.0	
	6Aβ_{9-40}	30.78	-21.53	-3.97	-22.53	8.94	-8.31	-6.8

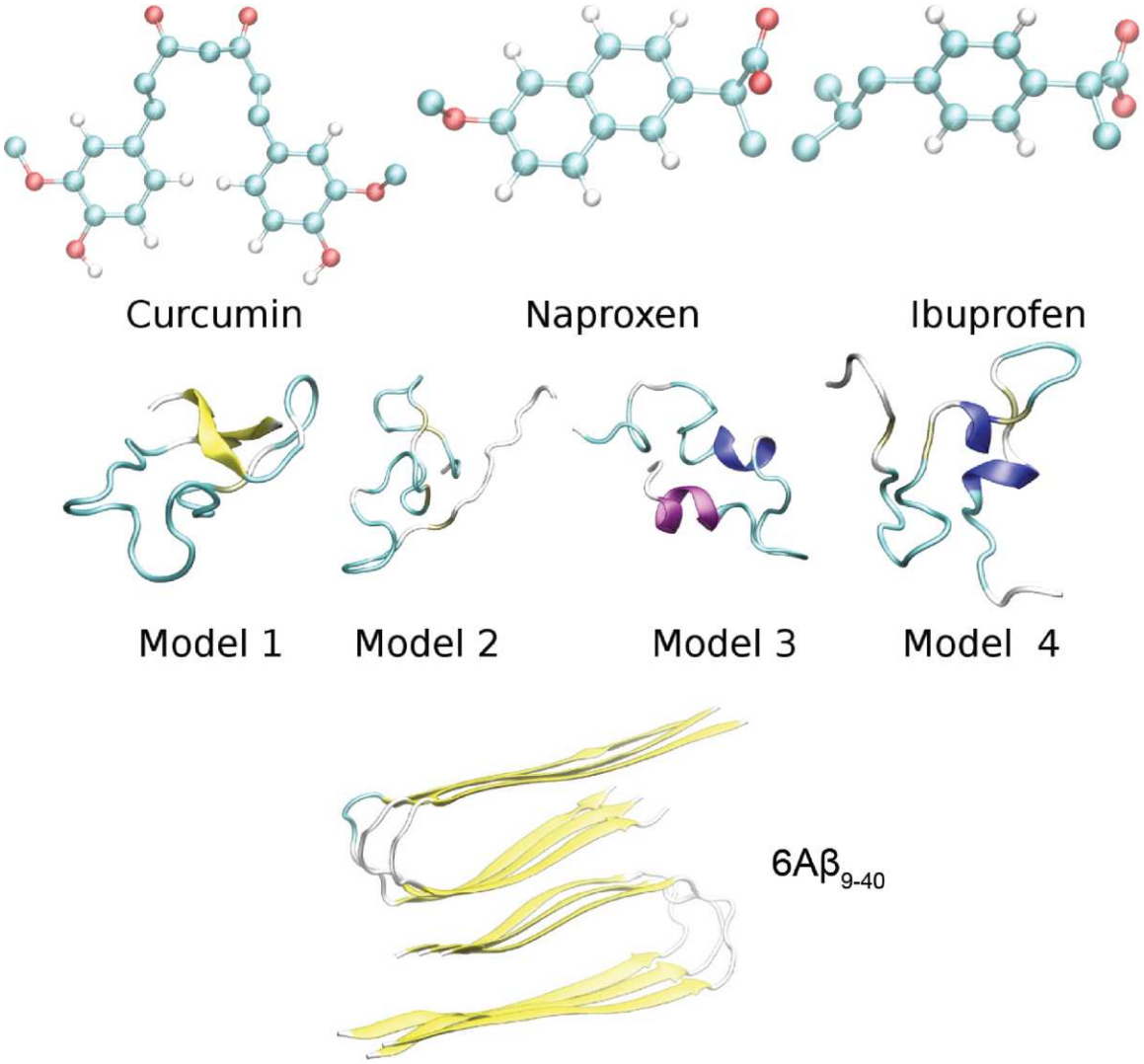

Figure 1: Chemical structures of curcumin, ibuprofen and naproxen (upper panel). Here we use the S-form of ibuprofen. Model 1 (middle panel) is the most populated structure obtained by CMD simulations starting from the random coil configuration for full length monomer Aβ_{40}. Model 2, 3, and 4 were obtained by REMD[51] for monomer. These 4 structures are used for the docking and MD simulations to estimate the binding free energy by the MM-PBSA method. The two-fold symmetric 6Aβ_{9-40} fibril structure, resolved by the solid state NMR technique[56] (bottom panel).

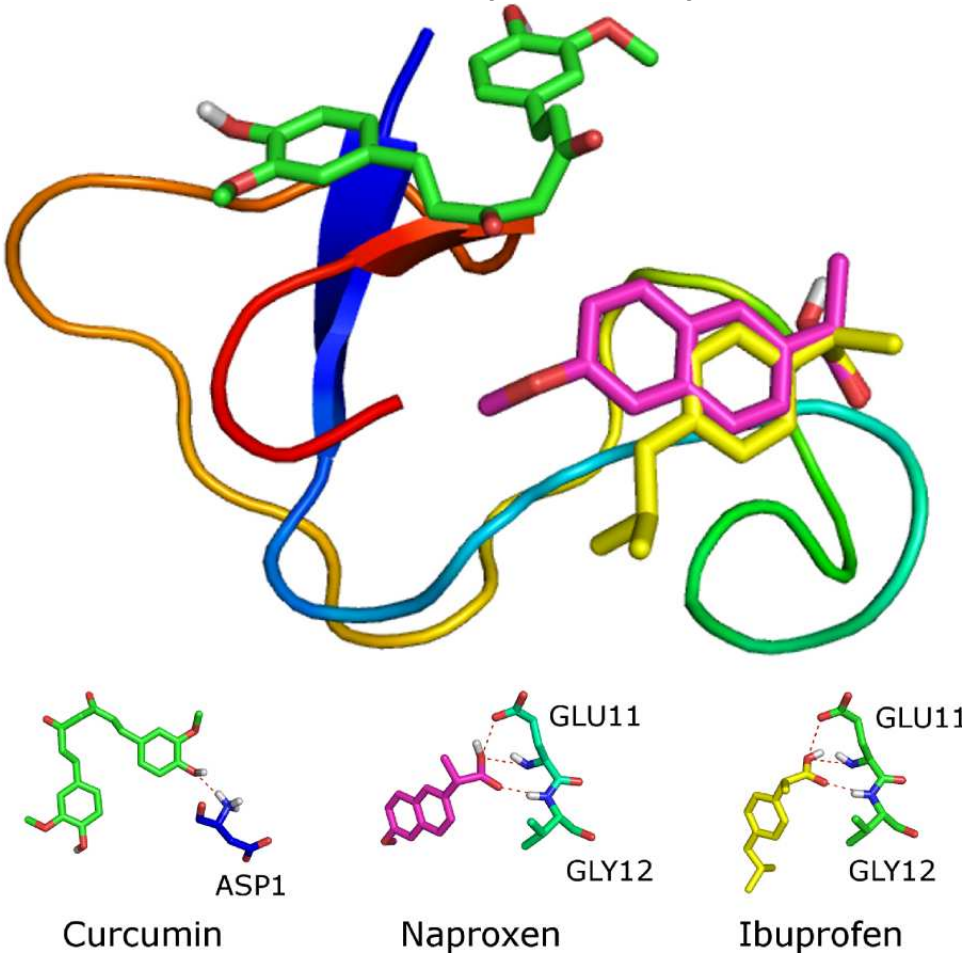

Figure 2: Binding sites of curcumin (green), naproxen (magenta), and ibuprofen (orange) obtained in the best docking mode for receptor Aβ_{1-40}-Model 1. The lower panel shows the HB networks for three ligands with the receptor.

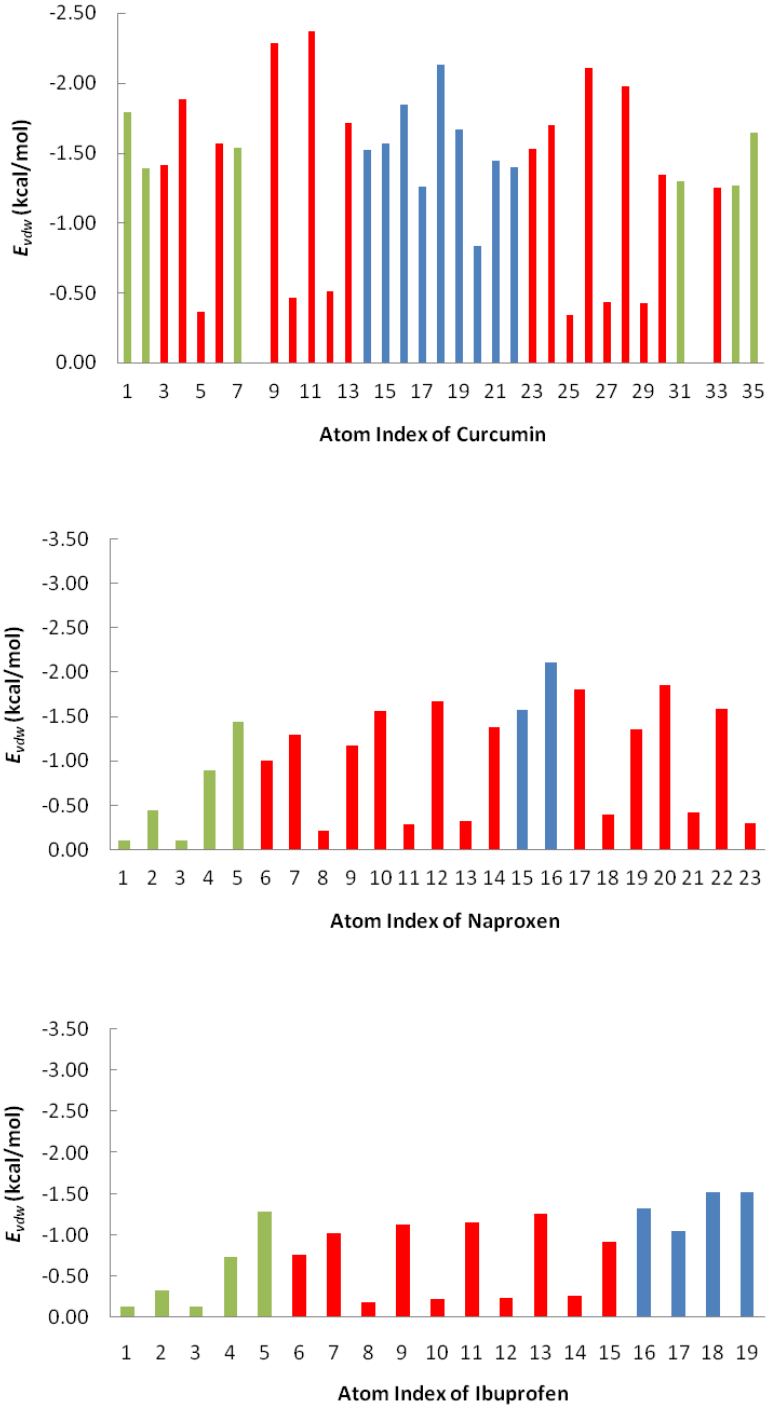

Figure 3: Contributions of individual atoms of three ligands to the vdW interaction energy. The results have been obtained in equilibrium for four models of monomer $A\beta_{1-40}$. Red color refers to atoms belonging to aromatic rings. For curcumin blue refers to atoms between two rings, while remaining atoms are in green. In the case of naproxen and ibuprofen blue and green indicate atoms on the left and right of aromatic rings, respectively.

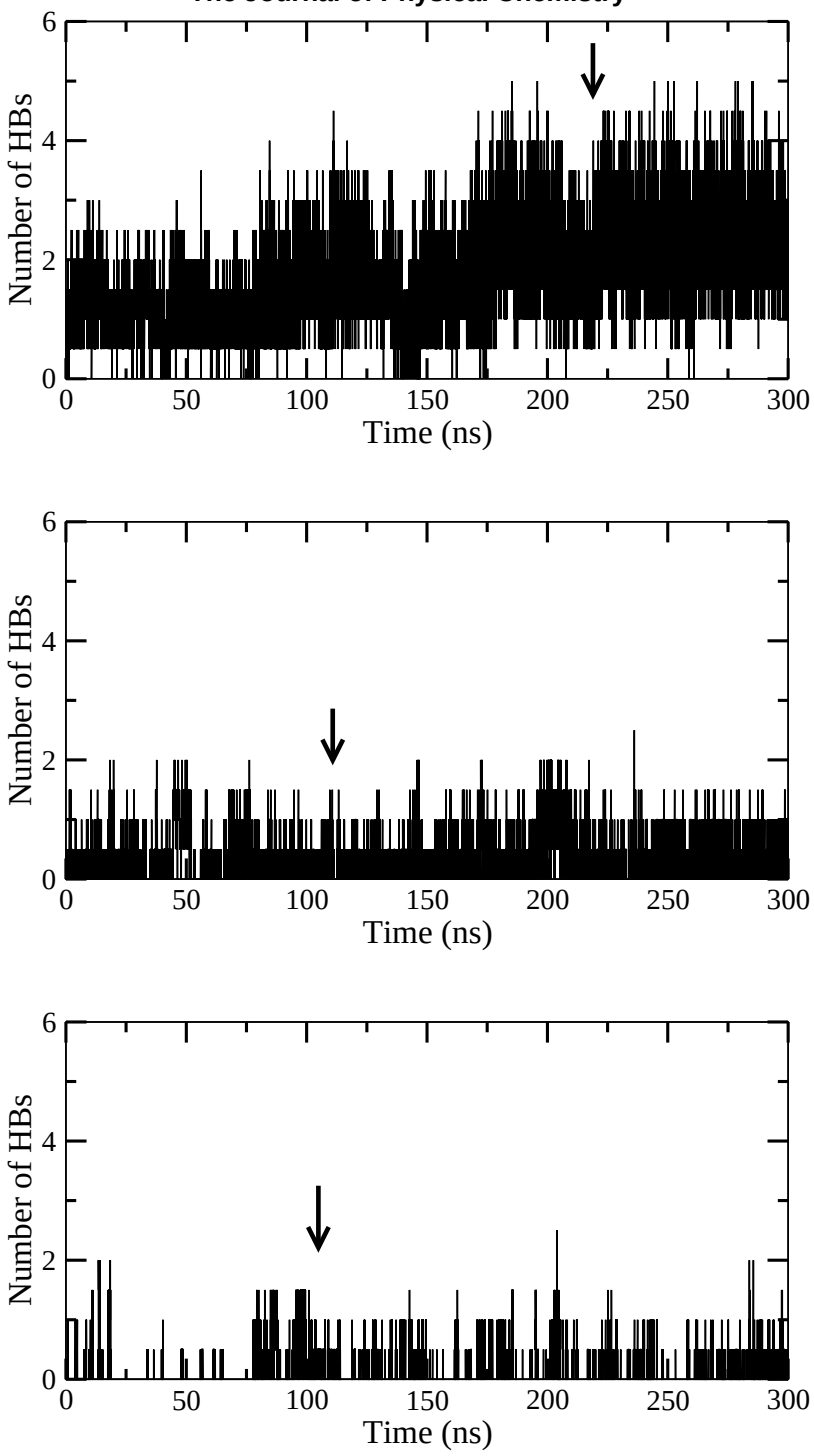

Figure 4: Time dependence of HBs between receptor Aβ_{1-40} and curcumin (upper), naproxen (middle) and ibuprofen (lower panel). The results have been obtained for Model 1. Arrows roughly refer to times when systems reach equilibrium. Using values of HBs collected in equilibrium (after arrows) we obtain the average $\overline{HB(t)}$ =2.34, 0.27, and 0.07 for curcumin, naproxen and ibuprofen, respectively.

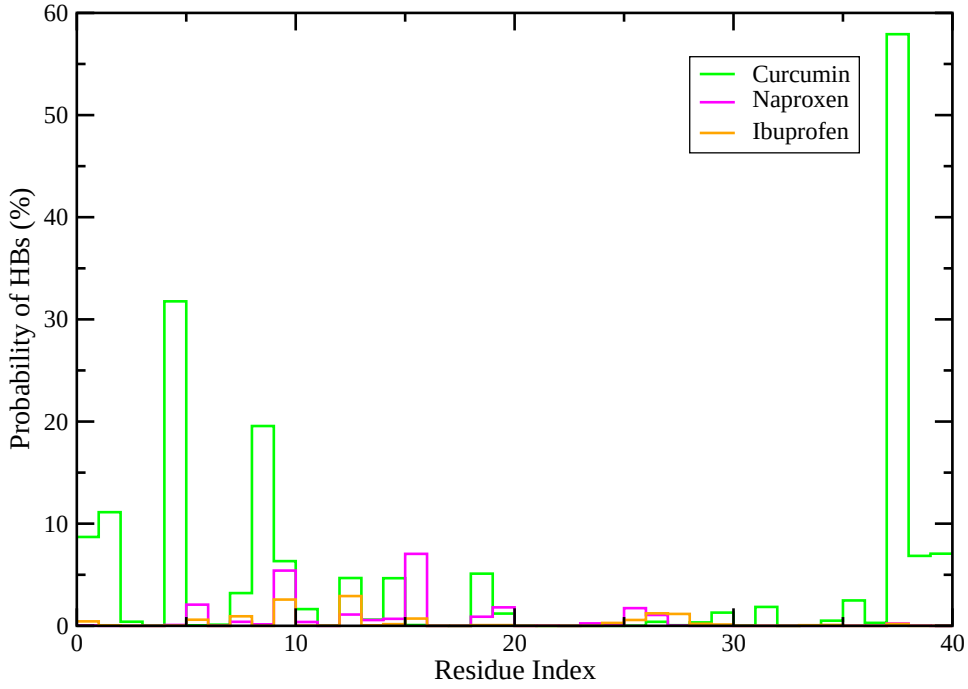

Figure 5: Probability of formation of HBs between curcumin, naproxen and ibuprofen and individual residues of Aβ_{1-40}-Model1. The results have been obtained from 300 ns MD simulations.

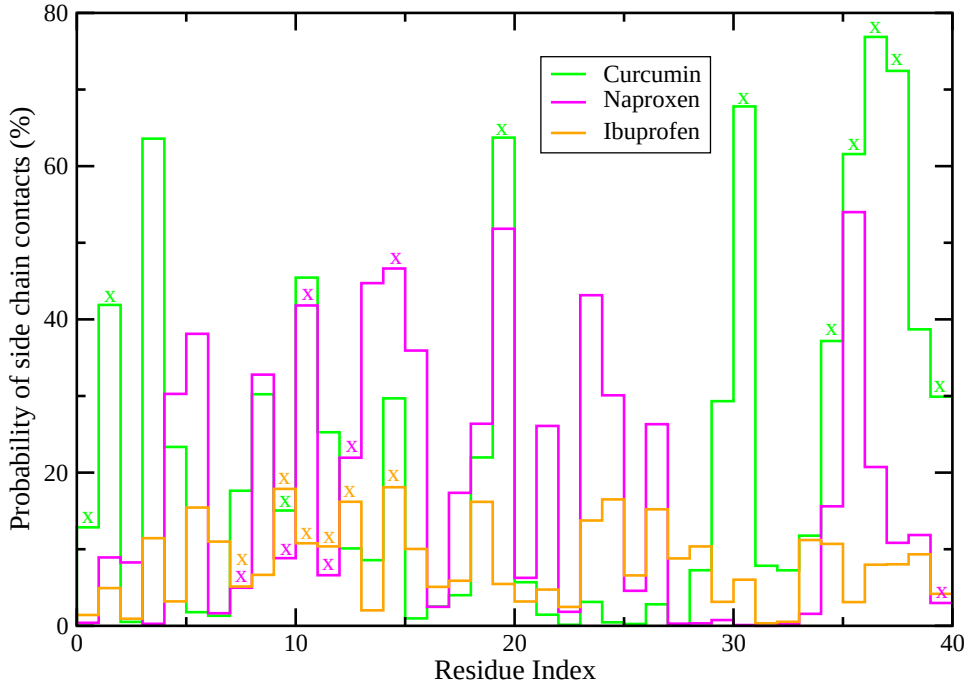

Figure 6: Probability of formation of SC contacts of curcumin, naproxen and ibuprofen with Aβ_{1-40}-Model 1. The results have been obtained from 300 ns MD simulations. Symbol X refer to those residues that have the SC with ligand in the best mode conformation obtained by the docking method (see Figure 2).

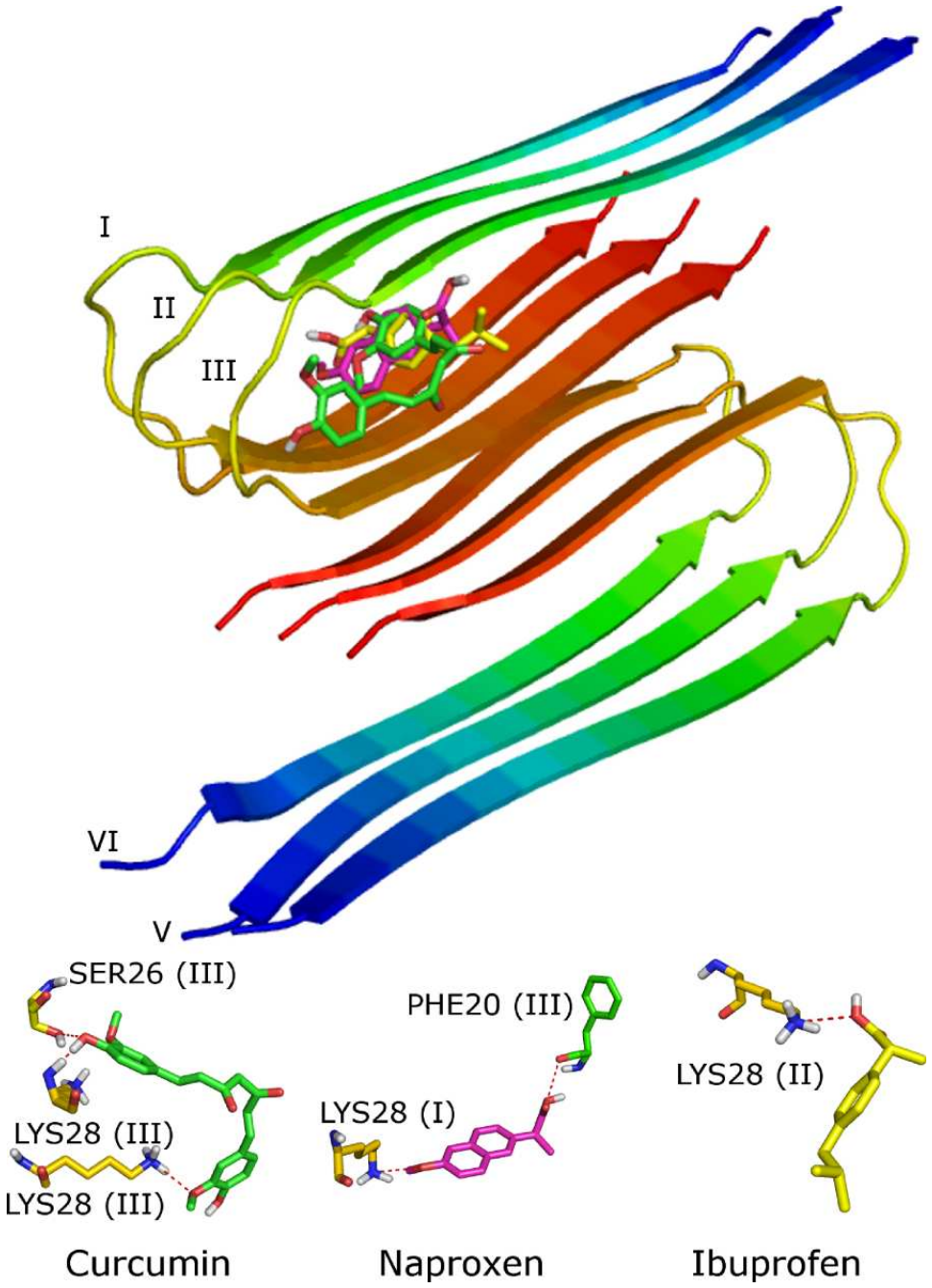

Figure 7: Binding sites of curcumin (green), naproxen (magenta) and ibuprofen (orange) to 2-fold symmetric 6Aβ_{9-40} fibril. The results were obtained in the best mode of docking. The lower panel shows the HB networks for curcumin, naproxen and ibuprofen.

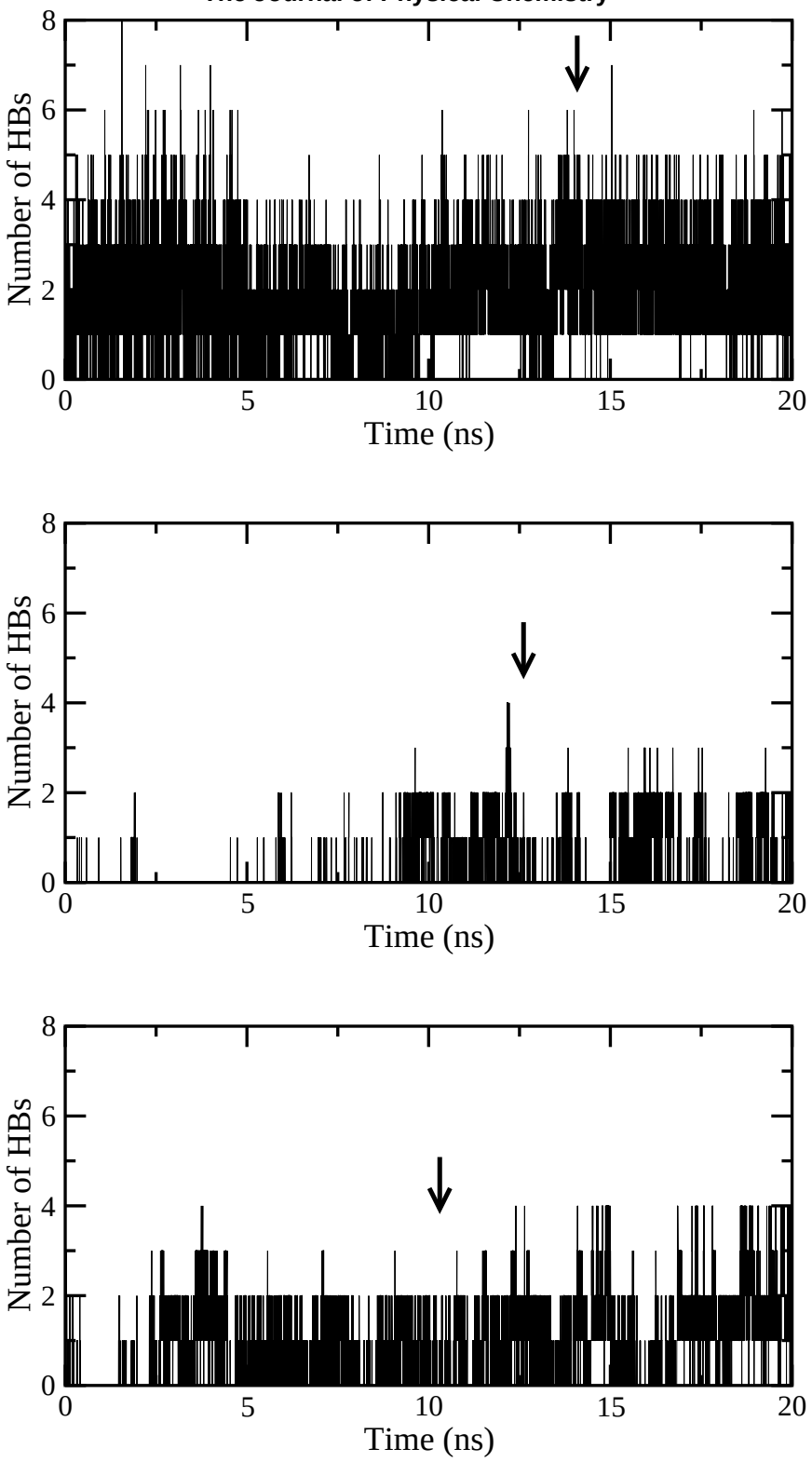

Figure 8: Time dependence of HBs between receptor 6Aβ_{9-40} and ligands curcumin (upper), naproxen (middle) and ibuprofen (lower panel). Arrows refer to times of reaching equilibrium (see Fig. S4). In equilibrium $\overline{HB(t)}$ =2.19, 0.56, and 1.21 for curcumin, naproxen, and ibuprofen, respectively.

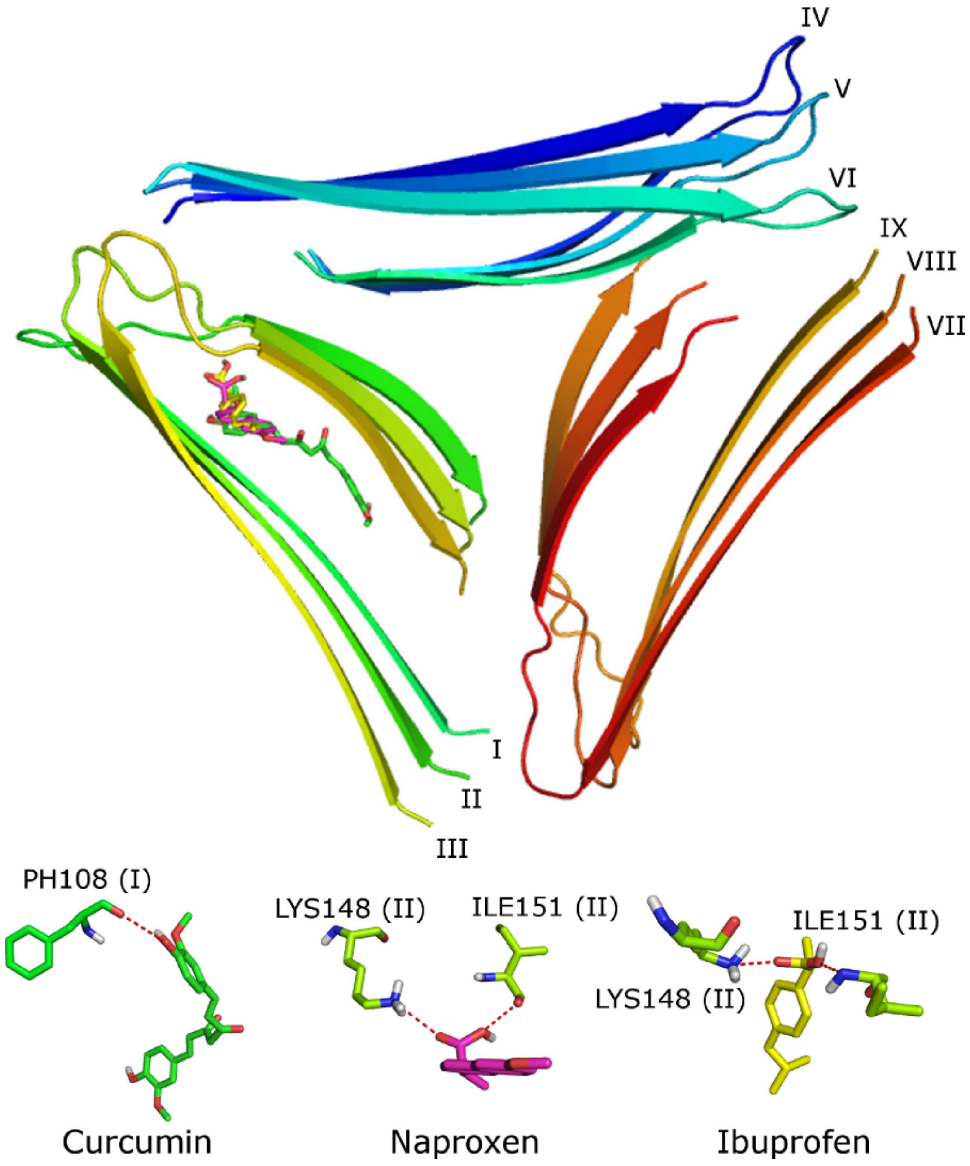

Figure 9: Binding sites of curcumin (green), naproxen (magenta) and ibuprofen (orange) to 3-fold symmetric 9Aβ_{9-40}. The results have been obtained in the best docking mode. The lower panel shows HB networks for three ligands with the receptor. Curcumin has one HB while naproxen and ibuprofen have two HBs.

Graphical TOC Entry